2023 IEEE Wireless and Microwave Technology Conference (WAMICON) | 979-8-3503-9864-9/23/$31.00 ©2023 IEEE | DOI: 10.1109/WAMICON57636.2023.10124900

Magnetic-Less Simultaneous Transmit and Receive Front End using Highly Efficient GaN-Based Quadrature Balanced Amplifier

Niteesh Bharadwaj Vangipurapu
INSPIRE Group
University of Central Florida
Orlando,USA
niteesh.bharadwaj9@knights.ucf.edu

Kenle Chen
INSPIRE Group
University of Central Florida
Orlando,USA
kenle.chen@ucf.edu

***Abstract*—This paper presents the first-ever high-power magnetic-less simultaneous transmit and receive (STAR) front end based on quadrature-balanced power amplifier (QB-PA). It is originally discovered that the harmonic-tuning and high output reflection of high-power GaN PA can be synergistically co-designed for achieving high TX efficiency and low receive (RX) path loss of the front end. Based on this methodology, a QB-PA-based STAR front end is practically designed using commercial GaN transistors as a proof-of-concept demonstration. The developed prototype experimentally achieves up to 80% PA efficiency at peak transmission power of 42.5 dBm and meanwhile very low receive loss of ≈ 1.5 dB. Moreover, STAR operation is experimentally conducted using both continuous and modulated TX stimulus at 1.6 GHz, in which a satisfactory reception performance is measured at 1.66 GHz with a very low RX EVM. This design radically outperforms the state-of-the-art by order of magnitude in TX power, together with significantly enhanced PA efficiency and antenna-interface efficiency.**

***Index Terms*—Balanced amplifier, continuous mode, full duplex, high efficiency, power amplifier, simultaneous transmit and receive, quadrature hybrid.**

I. Introduction

The transmission of wireless data has been of vital prominence and demands endless innovations. Along the technological evolution, the rapid surge in wireless data traffic have been increasingly making the spectrum very valuable and meanwhile a scanty resource. Our communication mechanisms, predominantly half-duplex, have necessitated the need for the full-duplex that have immediately doubled spectral efficiency and also offered many benefits at upper layers [1]–[3]. Full-duplex features simultaneous transmit and receive (STAR), which generally requires directional circulation of transmit (TX) and receive (RX) signals at the antenna interface.

Conventionally, the RF circulators are realized using magnetic materials making the resultant devices very bulky, expensive, and not integrable in a massive scale. The recent advances in spatial-temporal modulation have led to non-magnetic circulators, but these varactor/switch-based implementations are subject to intrinsically low power handling, high insertion loss, unsatisfactory linearity, etc [4]–[6]. Recently, quadrature-balanced power amplifier (QB-PA) has been utilized to realize

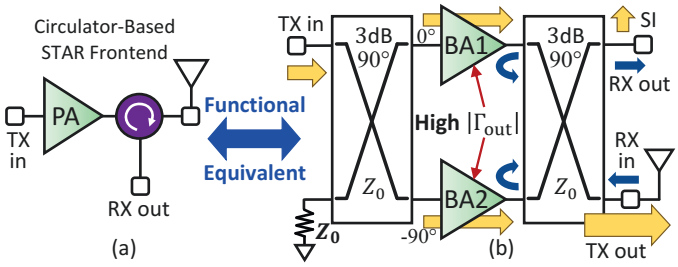

Fig. 1. Realization of STAR RF front end using: a) conventional circulator, b) GaN-based quadrature-balanced amplifier concurrently featuring high-power, magnetic-less, and high antenna-interface & PA efficiencies.

STAR front end, achieving promising full-duplex performance with properly designed self-interference cancellation (SIC) [7]. However, the reported QB-PA STAR front ends are still limited to low-power ($\leq$1 W) designs with low PA efficiency, and no systematic TX-RX co-design methodology has been studied.

This paper presents, for the first time, a high power ($\geq$10 W) magnetic-less STAR front end using GaN-based QB-PA, as illustrated in Fig. 1. For the transmission of the signal, the proposed front end can be deployed as a highly efficient amplifier while spontaneously being able to receive the signal with low loss and excellent linearity. It is revealed that the harmonic-tuned PA design can be well synergized with high reflection of PA output that culminates in an effective reconstruction of the receive signal at the output coupler's isolation port designated for reception. Upon the solid validation using a developed hardware prototype, the proposed method fundamentally unlocks the high-power operation of magnetic-less STAR front ends that has been a long-standing bottleneck. It thus exhibits a promising potential of pushing full-duplex/STAR from lab curiosity to realistic high-power radio systems.

II. Quadrature-Balanced Magnetic-Less Simultaneous Transmit and Receive Front End

A quadrature balanced amplifier, utilized here as a STAR front end, is presented in the Fig. 1. In the TX path, the input

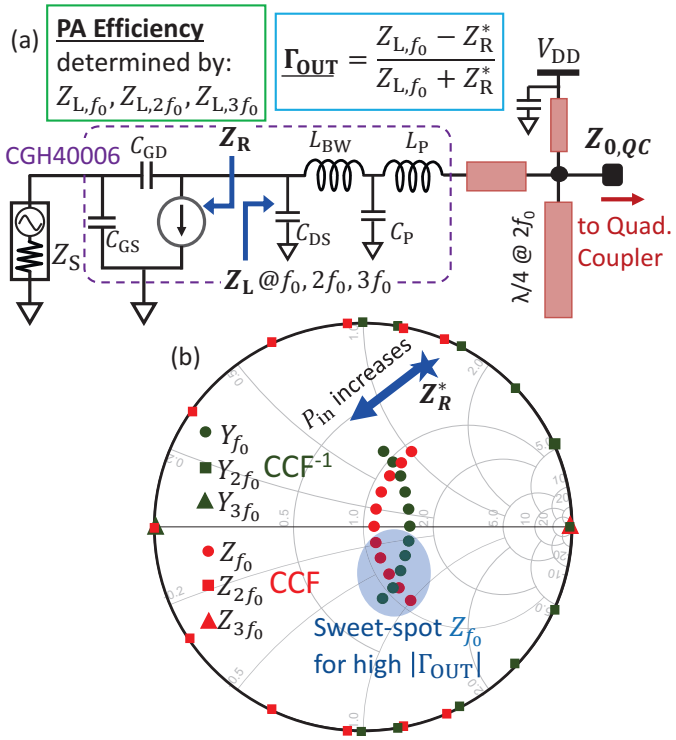

Fig. 2. PA design considerations for concurrently achieving high efficiency and high $|\Gamma_{\mathrm{out}}|$: a) schematic, b) optimal loadline choice.

TX signal splits at the first quadrature hybrid into BA1 and BA2, gets amplified and in-phase combined at the antenna port through the second quadrature hybrid. In the RX path, the received signal is split by the output quadrature hybrid, reflected by BA1 and BA2 output ports, and re-combined at the isolation port. At this RX terminal, the BA1 and BA2 output signals should be ideally cancelled, while the remaining leakage due to the realistic imperfections remain as self interference (SI) for RX. For this application, the design of each PA in this balanced topology should aim at achieving both high efficiency for efficient transmission and high output reflection (Γ_{out}) for low RX path loss.

A. Design of Continuous-Mode GaN PA with High $|\Gamma_{\mathrm{out}}|$

The design of high efficiency GaN PA has been very sophisticated throughout the past decade, and the most critical aspect is the choice of PA mode and loadline. Among the high-efficiency PA modes, continuous Class-F (CCF) and continuous Class-F^{-1} (CCF^{-1}) are the mostly commonly used for both the high efficiency and broadly extended design space. Realizing high-efficiency CCF and (CCF^{-1}) PAs require accurate loadline setting at fundamental frequency (f_0) but also cooperative harmonic engineering at $2f_0$ and $3f_0$. On the other hand, as depicted in Fig. 2(a), Γ_{out} of PA is determined by the mismatch between the fundamental loadline impedance (Z_{L,f_0}) and the reverse impedance looking backward to the drain of transistor (Z_{R}), i.e., the distance between Z_{R}^* and Z_{L,f_0} on the Smith chart.

A commercial GaN transistor, Wolfspeed CGH40006P, is examined for this design. Its corresponding CCF and CCF^{-1} loadline impedances at intrinsic current-generator plane are plotted in Fig. 2(b), where Z_0 of the Smith chart is set to R_{OPT}. The Z_{R}^* of the transistor is also extracted from large-signal simulation as indicated on the Smith chart. Note that Z_{R} at intrinsic drain is capacitive due to the feedback parasitic capacitor C_{GD} and gate capacitor C_{GS}, leading to an inductive Z_{R}^*. This impedance is also modulated by the input power and travels along the blue trajectory indicated on the Smith chart in Fig. 2(b). As a result, it becomes apparent that the capacitive loadlines of CCF and CCF^{-1} modes at the lower half plane of Smith chart presents the sweep-spot for realizing a high-$|\Gamma_{\mathrm{out}}|$ continuous-mode PA. Meanwhile, due to the modulation of Z_{R}^*, $|\Gamma_{\mathrm{out}}|$ is also power-dependent. Furthermore, given the finite isolation between drain and gate, the selection of input source impedance, Z_{S}, is important for further increasing $|\Gamma_{\mathrm{out}}|$. Thus, the overall design of individual PA in the balanced topology needs to consider all the aspects mentioned above to achieve a globally optimal balance between PA efficiency and RX loss.

B. Practical Harmonic-Tuned Design

A simplified harmonic-tuning network is realized together with fundamental matching provided by the quadrature coupler as a transformer, as shown in Fig. 2(a). In this design, a capacitive CCF^{-1} loadline is chosen which correspondingly requires an inductive second harmonic impedance that is properly set by an open-ended quarter-wave line ($@2f_0$)in conjunction with a tuning line. The fundamental matching is then realized using the coupler-transformer in parallel with the bias line as a shunt inductor. The third harmonic matching is usually more forgiven for a practical GaN transistor, which is only loosely tuned based on the existing OMN topology. The transformer-coupler is realized using a single-stage branch-line hybrid designed at 1.6 GHz, which is also the center frequency of harmonic-tuned PA.

After the initial OMN design, a global optimization of PA efficiency and RX loss is performed after connecting two sub-PAs with the quadrature coupler into a balanced topology. Fig. 3 shows the simulation results of the design QB-PA as a STAR front end. For TX performance, a high saturation efficiency up to 80% is achieved at 1.6 GHz. Simultaneous to TX operation, the basic RX performance is evaluated at a slighted deviated frequency at 1.66 GHz. As the simulation results shown in Fig. 3, a low RX loss (red dashed line) of < 2 dB is achieved up to saturation.

III. Implementation of Quadrature-Balanced Frontend Prototype

The designed quadrature-balanced frontend at 1.6 GHz is accomplished using commercial GaN devices (CGH40006P) for both the amplifier branches. The input quadrature coupler of QB-DPA is implemented using a standard 3-dB branch-line hybrid, and the output stage is designed using the harmonic-tuned schematic shown in Fig. 4.The designed amplifier stage

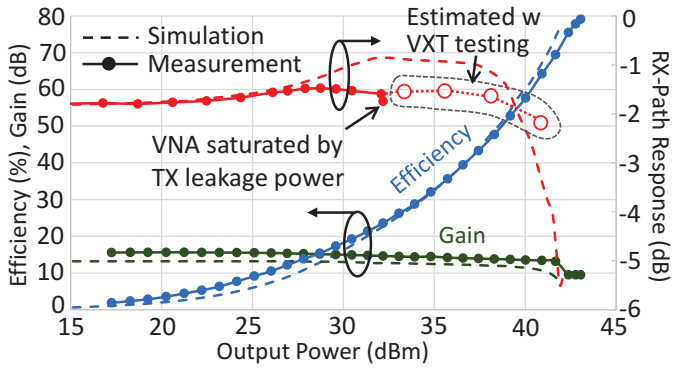

Fig. 3. Simulation and measurement results of basic TX and RX performance of the designed QB-PA STAR front end.

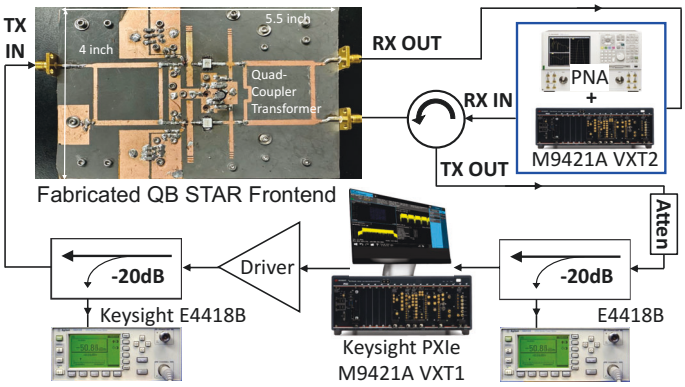

Fig. 4. Experimental setup for testing the fabricated QB-PA STAR front end.

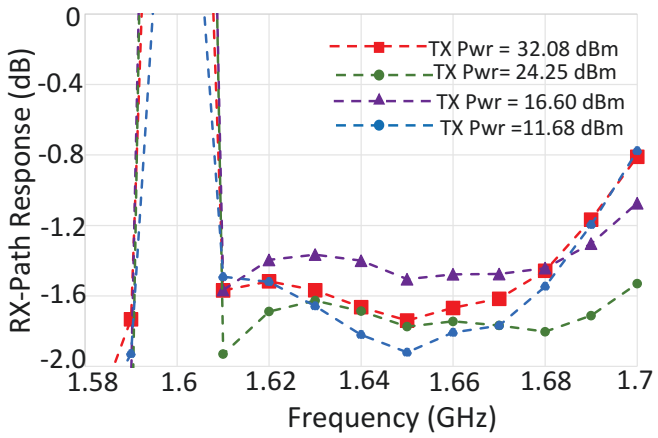

Fig. 5. Measurements of the RX path response to CW signals of various power levels as a function of receiving signal frequency.

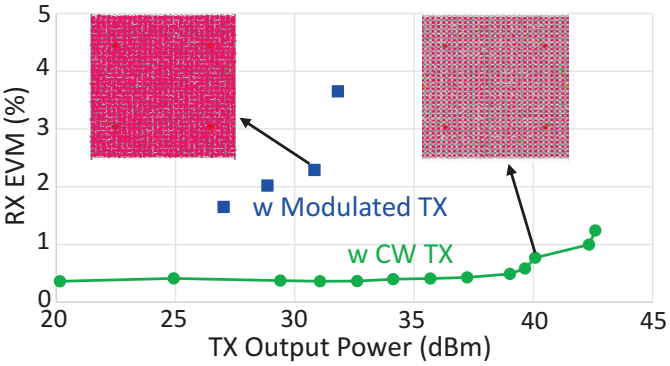

Fig. 6. RX linearity measurement with CW and modulated TX stimuli. (TX Modulation: 4GLTE, 1.6 GHz, 20 MHz, 256QAM, 10.5-dB PAPR, RX Modulation: 5GNR, 1.66 GHz, 40 MHz, 1024QAM)

manifests itself as a full duplex system with appealing characteristics that enable the STAR. The design is aimed for deliverables like high efficiency and low receiver loss at a high power that distinguishes the presented design from state-of-the-art. Consequently, the design of the matching network with requisite electrical lengths is carried out thus ensuring a functional prototype. The designed prototype of the high power RF front-end is fabricated on a 20-mil thick Rogers Duroid-5880 PCB board with dielectric constant of 2.2 for implementation at frequency of 1.6GHz as shown in the Fig. 4. The RX path loss was measured using a Network Analyzer, in a test at which the TX is feeding in the signal at various power levels at 1.6 GHz at to actuate a real FD environment. The transmit signal was generated and fed to the TX using Keysight PXIe.

IV. Experimental Results

Using the measurement setup in Fig. 4, the developed QB-PA STAR front end is first evaluated by simultaneously operating TX and RX with continuous-wave (CW) excitation. In the transmission path, the designed CCF^{-1} GaN PAs are equally biased in Class-AB region, and the drain supply voltages are set to 28 V for BAs to ensure an efficient performance. A high PA efficiency of around 80% at a peak power of 42 dBm are measured, as the results shown Fig. 3. The response of reception path is first measured using a Keysight performance network analyzer (PNA). A low path loss of around 1.6 dB is measured up to 32 dBm, where the PNA receiver with limited dynamic range is saturated by the TX leakage power. At higher TX power, the RX loss is estimated from the testing using Keysight Vector Transceiver (VXT) with a much higher dynamic range, which indicates a sustained low RX loss up to the QB-PA saturation. The frequency response of RX path response is also plotted in Fig. 5 under different TX power levels, indicating a consistently low RX loss across the frequency range from 1.62 to 1.7 GHz.

As an important RX characteristic, the linearity of RX path is further evaluated, in which a 40-MHz bandwidth 5G signal at 1.66 GHz is applied at the input of the receiver along with TX power being fed into the PA. First, the TX is stimulated with a power-swept CW signal at 1.6 GHz, and a highly linear receiver path response is measured with very low EVM ($< 2\%$) up to the peak TX power of 42 dBm, as shown in Fig. 6. It is important to note that the TX leakage, though slightly deviated from the RX in frequency domain, is sufficiently low due to the cancellation of quadrature coupler, which does not affect the testing equipment of VXT. Sec-

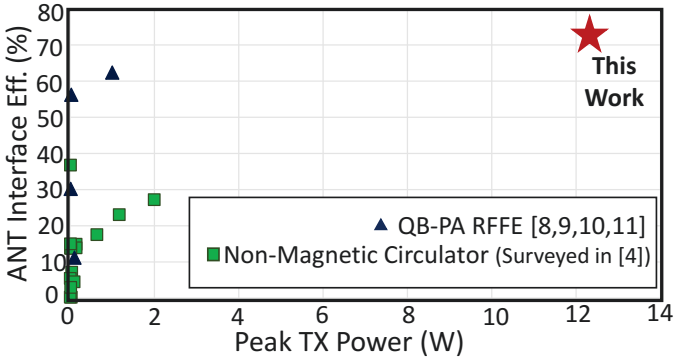

Fig. 7. Comparison with stat-of-the-art non-magnetic STAR front ends.

ond, the receiver linearity is measured with a 20-MHz LTE modulated signal being stimulated through the transmitting path, showing a good reception quality with EVM below 3.8% at various average TX power. The slight degradation of RX performance is mainly due to the increased noise floor of RX channel, which is adjacent to TX channel and affected by the TX spectrum regrowth due to non-linearity of QB-PA. This noise can be effectively cancelled through proper SIC designs as presented in [8].

To comprehensively evaluate the front end performance, a widely used figure of merit, i.e., antenna interface efficiency (η_{ANT}) [4], is calculated for this design and compared to state-of-the-art summarized in Fig. 7 including solutions based on both non-magnetic circulator [4] and QB-PA [8]–[11]. It is important to note that the operational peak TX power is greatly elevated from watt level to 10-watt level (an order of magnitude from state-of-the-art). Meanwhile, this design also demonstrates the highest-ever η_{ANT} of 72% which can be calculated according to the formula shown below [5]:

$$\eta_{ANT} = \frac{P_{out,PA} \times S_{21}/NF}{P_{out,PA}/\eta_{PA} + P_{DC,interface}} \times \frac{1}{\eta_{PA}} \times 100\%. \quad (1)$$

V. Conclusion

This paper presents the design and implementation of a magnetic-less and a high power Front end that can be fruitfully exploited for the purposes of long-range full duplex communications. It is, for the first time, proved that the GaN transistor can be designed as a well functional frontend offering very high efficiency and a very low receiver loss. As a proof-of-concept demonstration, a physical prototype based on quadrature-balanced platform is designed using GaN transistors. The proposed concept is validated by the functioning prototype with a state-of-the-art efficiency performance and appealing linearity response. To fully unleash the potential of the proposed STAR front end, advanced SIC designs will be performed to enable high-power in-band full-duplex communications.

References

[1] J. Zhou, T.-H. Chuang, T. Dinc, and H. Krishnaswamy, "Integrated wideband self-interference cancellation in the rf domain for fdd and full-duplex wireless," *IEEE Journal of Solid-State Circuits*, vol. 50, no. 12, pp. 3015–3031, 2015.

[2] H. Abolmagd, R. Subbaraman, D. Bharadia, and S. Shekhar, "Full-duplex wireless for (joint-) communication and sensing," in *ESSCIRC 2022- IEEE 48th European Solid State Circuits Conference (ESSCIRC)*, 2022, pp. 542–545.

[3] J. Zhou, N. Reiskarimian, J. Diakonikolas, T. Dinc, T. Chen, G. Zussman, and H. Krishnaswamy, "Integrated full duplex radios," *IEEE Communications Magazine*, vol. 55, no. 4, pp. 142–151, 2017.

[4] A. Nagulu and H. Krishnaswamy, "Non-magnetic non-reciprocal microwave components — state of the art and future directions," *IEEE Journal of Microwaves*, vol. 1, no. 1, pp. 447–456, 2021.

[5] N. Reiskarimian, A. Nagulu, T. Dinc, and H. Krishnaswamy, "Non-reciprocal electronic devices: A hypothesis turned into reality," *IEEE Microwave Magazine*, vol. 20, no. 4, pp. 94–111, 2019.

[6] T. Dinc, A. Nagulu, and H. Krishnaswamy, "A millimeter-wave non-magnetic passive soi cmos circulator based on spatio-temporal conductivity modulation," *IEEE Journal of Solid-State Circuits*, vol. 52, no. 12, pp. 3276–3292, 2017.

[7] N. Ginzberg and E. Cohen, "Transceiver architectures for fully integrated frequency division duplex (fdd) systems with wideband tx interference cancellation," in *2020 IEEE Texas Symposium on Wireless and Microwave Circuits and Systems (WMCS)*, 2020, pp. 1–7.

[8] N. Ginzberg, D. Regev, G. Tsodik, S. Shilo, D. Ezri, and E. Cohen, "A full-duplex quadrature balanced rf front end with digital pre-pa self-interference cancellation," *IEEE Transactions on Microwave Theory and Techniques*, vol. 67, no. 12, pp. 5257–5267, 2019.

[9] E. Manuzzato, J. Tamminen, M. Turunen, D. Korpi, F. Granelli, and M. Valkama, "Digitally-controlled electrical balance duplexer for transmitter-receiver isolation in full-duplex radio," in *European Wireless 2016; 22th European Wireless Conference*, 2016, pp. 1–8.

[10] N. Ginzberg, D. Regev, R. Keren, and E. Cohen, "A 65 nm cmos quadrature balanced switched-capacitor power amplifier for full- and half-duplex wireless operation," *IEEE Journal of Solid-State Circuits*, vol. 56, no. 10, pp. 3008–3020, 2021.

[11] N. Ginzberg, D. Regev, R. Keren, S. Shilo, D. Ezri, and E. Cohen, "A four-element 5–6-ghz cmos quadrature balanced full-duplex mimo transmitter with wideband digital interference cancellation," *IEEE Microwave and Wireless Components Letters*, vol. 32, no. 2, pp. 173–176, 2022.